Internal Mg^{2+} block of recombinant NMDA channels mutated within the selectivity filter and expressed in *Xenopus* oocytes

Jürgen Kupper, Philippe Ascher and Jacques Neyton

Laboratoire de Neurobiologie (URA CNRS 1857) Ecole Normale Supérieure, 46 rue d'Ulm, 75005 Paris, France

(Received 31 July 1997; accepted 14 October 1997)

1. The NMDA receptor channel is blocked by both external and internal Mg^{2+} ions, which are assumed to bind inside the channel on each side of a central barrier. We have analysed the internal Mg^{2+} block in recombinant NR1–NR2A NMDA receptors expressed in *Xenopus* oocytes. We have determined the effects of mutations of two asparagines that line the selectivity filter of the channel, one located within the NR1 subunit (N598) and the other within the NR2A subunit (N596).

2. The whole-cell current–voltage relation of wild-type NMDA channels shows inward rectification that reflects the voltage-dependent block produced by the internal Mg^{2+} of the oocyte. This inward rectification is slightly reduced in the NR2 mutant (N596S) but is abolished in the NR1 mutants (N598Q and N598S). This suggests that the NR1 asparagine plays a larger role than the NR2 asparagine in controlling the internal Mg^{2+} block.

3. Single-channel current–voltage relations confirm that the internal Mg^{2+} block is reduced in both the NR1 and NR2 mutants. However, the reduction is small and is similar for the two families of mutants.

4. The discrepancy between whole-cell and single-channel data is partly due to differential effects of internal Mg^{2+} on the open probabilities of the two conductance states present in NR1 mutant channels.

5. The results suggest that mutations of NR1 and NR2 asparagines lower the central barrier to Mg^{2+}. An additional contribution of the NR2 asparagine to the external Mg^{2+} binding site (and possibly to the external barrier that controls access to this site) may account for the marked relief of external Mg^{2+} block produced by the NR2 mutation.

Extracellular Mg^{2+} block is a key functional property of the *N*-methyl-D-aspartate (NMDA) receptor channel that accounts for the regenerative properties of the NMDA responses and underlies the requirement for simultaneous binding of agonist and membrane depolarization for channel opening. Early studies of Mg^{2+} block suggested Mg^{2+} binding to a site situated deep in the channel (Nowak, Bregestovski, Ascher, Herbet & Prochiantz, 1984; Mayer, Westbrook & Guthrie, 1984; Ascher & Nowak, 1988; Jahr & Stevens, 1990). Further studies demonstrated that NMDA channels are also blocked by internal Mg^{2+}, with a voltage dependence opposite to that of the external Mg^{2+} block, implicating the existence within the channel of two separate Mg^{2+} binding sites separated by a central barrier (Johnson & Ascher, 1990; Li- Smerin & Johnson, 1996*a*).

The molecular identification of the central barrier and of the two Mg^{2+} binding sites remains incomplete. After the cloning of the various NR1 and NR2 subunits of the NMDA channel, site-directed mutagenesis studies rapidly implicated two asparagine residues situated within the second hydrophobic segments (M2): NR1(N598) and NR2(N595), which we will call NR1(N0)) and NR2(N0), respectively (Burnashev *et al.* 1992; Mori, Masaki, Yamakura & Mishina, 1992; Sakurada, Masu & Nakanishi, 1993). Mutations of either asparagine alter external Mg^{2+} block, but the effects of mutating NR1(N0) are less profound than those produced by mutating NR2(N0) (Burnashev *et al.* 1992). Further studies revealed that NR1(N0) and NR2(N0) residues are probably staggered relative to one another, and that in the pore (within the proposed selectivity filter domain), NR1(N0) faces N596 of the NR2A subunit, called NR2(N+1) (Wollmuth, Kuner, Seeburg & Sakmann, 1996; Kuner, Wollmuth, Karlin, Seeburg & Sakmann, 1996). Mutations of NR2(N+1), like those of NR2(N0), strongly alter external Mg^{2+} apparent affinity (Kupper, Ascher & Neyton, 1996).

The present study was originally designed to determine whether mutations of the asparagine residues forming the selectivity filter of NMDA receptors also affect the block by internal Mg^{2+} ions. We analysed the effects of three

mutations, one of NR2A(N+1) and two of NR1(N0). Preliminary results obtained on currents recorded in whole oocytes suggested that the mutation of NR2A reduced mostly the external Mg^{2+} block, whereas the mutations of NR1 preferentially reduced the internal Mg^{2+} block. However, further study at the level of single-channel current recording revealed that NR2 and NR1 mutations produced quite similar, and rather limited, reductions of internal Mg^{2+} block. The apparent changes in Mg^{2+} block of the macroscopic currents in the NR1 mutants actually reflect changes in the probability of opening of the channels, and in particular an alteration of the relative open probabilities of the two conductance states found in the mutant channels.

METHODS

Expression of mRNA in *Xenopus* oocytes

The preparation of oocytes was carried out as described in Bertrand, Cooper, Valera, Rungger & Ballivet (1991). Before removing the oocytes, the animals were anaesthetized in an ice bath containing 0·2% MS-222 for 20 min. pcDNA3 expression plasmids used in this study have been described previously (Kupper *et al.* 1996). To facilitate comparisons with other studies we have adopted the nomenclature proposed by Kuner *et al.* (1996) for single amino acid mutations in the M2 region of the NMDA subunits. Accordingly, as mutant NR1 subunits were co-expressed with wild-type NR2A subunits and vice versa, mutant channels containing one of the three mutations analysed in this study, NR1(N598Q), NR1(N598S) and NR2A(N596S), will be referred to as NR1(N0Q)–NR2A, NR1(N0S)–NR2A and NR1–NR2A(N+1S), respectively. To generate cRNA, we linearized plasmids with *Xba*I and utilized the T7 mMessage mMachine Kit according to the manufacturers instructions (Ambion, Austin, TX, USA). Approximately 10–50 ng of NR1 and NR2A cRNAs were mixed at a ratio of 1:3 and co-injected into each oocyte. Within 24 h of cRNA injection non-desensitizing glutamate-activated whole-cell currents of between 1 and 5 μA (−80 mV, no external Ca^{2+}) were readily obtained.

Recording conditions

Patch pipettes, prepared from borosilicate glass (Assistent, Hilgenberg, Germany), ranged from 1·5 to 7 MΩ resistance when filled with a solution containing (mM): 112 CsCl, 10 Hepes and 10 BAPTA (pH 7·2; titrated with about 38 mM CsOH). Mg^{2+}-containing solutions were prepared by addition of 5·11 mM $MgCl_2$ to the pipette solution to yield a free Mg^{2+} concentration of 4 mM as calculated with the WinMaxc program kindly provided by Chris Patton (Bers, Patton & Nuccitelli, 1994). For the experiments using asymmetric monovalent ionic solutions, Cs^+ in the pipette solution was replaced by K^+ and Cs^+ in the external perfusion solutions was replaced with Na^+.

Outside-out patches were formed from oocytes superfused with a solution containing (mM): 140 NaCl, 2·8 KCl, 1 $CaCl_2$ and 10 Hepes (pH 7·2 adjusted with NaOH). After obtaining a stable patch, the pipette was moved into the stream of a double-barrelled perfusion system containing various external solutions. One barrel typically contained (mM): 147 CsCl, 10 Hepes (pH 7·2 adjusted with CsOH) and glycine (10 or 100 μM). To activate single channels, patches were exposed to the other barrel which contained the same solution plus glutamate (10 or 100 μM).

Two types of outside-out patches were used. For measuring single-channel conductances, oocytes with a moderate expression level (1–4 μA at −100 mV and in the presence of 100 μM glutamate and 10 μM glycine) were selected. The membrane was brought from a holding potential of −60 mV to test potentials ranging from −100 to +100 mV in steps of 10 or 20 mV while the patch was perfused with the 10 μM glutamate solution. For measuring macroscopic patch currents in an extended potential range, patches were taken from oocytes with high levels of channel expression (>10 μA under the same screening conditions). The two barrels contained 100 μM glycine with or without added glutamate (100 μM). The membrane potential of the patch was held at −50 mV and periodically varied from −150 to +200 mV by the application of 3 s ramps. In some experiments with NR1(N0Q)–NR2A and NR1(N0S)–NR2A channels we added 100 μM EDTA in the external solutions to chelate traces of Ca^{2+} ions, as Ca^{2+} blocks the mutant channels studied with high affinity (Burnashev *et al.* 1992; Ruppersberg, Mosbacher, Günther, Schoepfer & Falker 1993; Premkumar & Auerbach, 1996).

External Mg^{2+} block was assessed from macroscopic 'whole-oocyte' currents using two-electrode voltage-clamp and voltage-ramp protocols as described in our previous study (Kupper *et al.* 1996). To avoid activation of Ca^{2+}-induced currents endogenous to the oocyte (at potentials above +50 mV), 100 μM EGTA was present in the external solutions containing (mM): 100 NaCl, 2·5 KCl, 10 Hepes (pH adjusted to 7·6 with NaOH).

All experiments were conducted at room temperature (20–22 °C).

Data acquisition and analysis

Single-channel currents were recorded with an Axopatch 200A amplifier (Axon Instruments), low-pass filtered at 2 kHz with an 8-pole Bessel filter and sampled at 5 kHz. Records were acquired and analysed with the Strathclyde Electrophysiological software (John Dempster, University of Strathclyde, Glasgow, UK). For NR1–NR2A wild-type and NR1–NR2A(N+1S) channels, which open primarily to a single conductance state, amplitude histograms at each membrane potential were usually constructed from a minimum of 100 transitions detected with a 50% threshold crossing routine. For NR1(N0Q)–NR2A and NR1(N0S)–NR2A channels, which open to two conductance levels, single-channel current values were determined by fitting Gaussian curves to all point amplitude histograms using the least squares fitting procedure of the software Origin 4.0 (Microcal, Northampton, MA, USA). For a three-state (main, sub and closed) channel, eqn (1) was used in the fitting procedure:

$$y = \sum_{i=1}^{i=3} \left(\frac{A_i}{w_i \sqrt{(\pi/2)}} e^{-2(x-x_i)^2/w_i^2} \right), \quad (1)$$

in which A_i is the total area under the ith peak, w_i corresponds to 2 'sigma', i.e. approximately 0·849 the width of the ith peak at half-height, and x_i is the amplitude of the centre of the ith peak.

Because in different experiments the single-channel amplitudes of recombinant NMDA channels detected under apparently identical conditions are variable (Béhé, Stern, Wyllie, Nassar, Schoepfer & Colqhoun, 1995), we normalized all our data to the current values at −100 mV, where the block by 4 mM internal Mg^{2+} is negligible.

Macroscopic patch currents were sampled at 500 Hz and low-pass filtered at 100 Hz with an 8-pole Bessel filter. Leakage currents and capacitive transients were recorded while the patch was exposed to the barrel lacking glutamate and subtracted from test records.

Three to five test records were bracketted by at least two leakage records. Test records were accepted only if the leakage records obtained before and after the test records were superimposable.

Current responses from 'whole oocytes' were recorded with a 725-A oocyte-clamp (Warner Instruments, Hamden, CT, USA), low-pass filtered at 100 Hz, sampled at 250 Hz and analysed using the pCLAMP 6 software (Axon Instruments).

Additional analyses of single (i) and macroscopic (I) current amplitudes utilized Origin 4.0 (Microcal). The unblocked fraction of the current (UF) was obtained by dividing the mean amplitude of currents recorded in the presence of internal (or external) Mg^{2+} (i_{Mg} or I_{Mg}) by the mean amplitude of currents recorded in the absence of Mg^{2+} (i_0 or I_0). The variations of UF as a function of voltage showed that UF did not tend towards zero at extreme potentials (high negative potentials in the case of external Mg^{2+} block; high positive potentials in the case of internal Mg^{2+} block). This suggested the possibility of a permeation of the blocking ion through the channel (see Discussion).

To model the voltage dependence of UF for internal Mg^{2+} block, we assumed that the energy profile for Mg^{2+} ions within the channel can be represented by a three-barrier two-site model. Mg^{2+} permeation is proposed to be limited by a central energy barrier that is higher than either of the more superficial energy barriers. Given this profile, Mg^{2+} ions entering the pore from either the external or the cytoplasmic compartment will block the channel by binding to the first site encountered (external or internal, respectively). Mg^{2+} will dissociate from this site and transit either back to the compartment of origin (unblocking) or through the pore towards the other compartment (permeation). As the latter route comprises the highest barrier, we assume this step is rate limiting throughout the entire experimental voltage range. Therefore, for the study of internal block, the 3B2S model can be reduced to a 2B1S model for which we can use the Woodhull formalism (Woodhull, 1973) leading to eqn (2):

$$\mathrm{UF} = \frac{k_{\mathrm{off}} e^{(-z\delta_{\mathrm{off}}\Phi V)} + k_{\mathrm{perm}} e^{(z\delta_{\mathrm{perm}}\Phi V)}}{k_{\mathrm{off}} e^{(-z\delta_{\mathrm{off}}\Phi V)} + k_{\mathrm{perm}} e^{(z\delta_{\mathrm{perm}}\Phi V)} + [Mg^{2+}] k_{\mathrm{on}} e^{(z\delta_{\mathrm{on}}\Phi V)}}, \quad (2)$$

in which z, F, R, T and V have their usual meanings, $\Phi = F/RT$, and $[Mg^{2+}]$ is the internal Mg^{2+} concentration. The rate constants for blocking, unblocking and permeation for internal Mg^{2+} ions at 0 mV are referred to as k_{on}, k_{off} and k_{perm}, respectively. The value of k_{on} is defined by the height of the energy barrier at the internal face of the channel, the value of k_{off} by the energy difference between the height of this barrier and that of the neighbouring energy well, and the value of k_{perm} by the energy difference between this 'internal' well and the central barrier. δ_{on}, δ_{off} and δ_{perm} are the apparent fractions of membrane field felt by the internal Mg^{2+} in the blocking, unblocking and permeation processes.

Experimental values are given as means ± S.D.

RESULTS

Whole-oocyte I–V relations of wild-type and mutant NMDA channels: comparison of the external and internal Mg^{2+} blocks

Figure 1*A–D* shows four pairs of I–V curves obtained during glutamate application from oocytes expressing either wild-type channels (*A*) or one of the three mutant NMDA channels as noted (*B*, *C* and *D*). Each graph shows two superimposed current traces obtained with voltage ramps from −150 to +100 mV in the same oocyte: one in the absence of external Mg^{2+} and the other one in the presence of external Mg^{2+} (100 μM). Comparison of the records in each case reveals the profound reduction of the external Mg^{2+} block in the mutant NR2(N+1) (*B*), and its persistence in the two mutants NR1(N0) (*C* and *D*). This asymmetry is in agreement with the observations of Burnashev *et al.* (1992). Quantification of the extent of block produced by external Mg^{2+} (Fig. 1*E*) further illustrates the unique properties of the NR2(N+1) mutant.

In the absence of external Mg^{2+}, the I–V relationship obtained from oocytes expressing NR1–NR2A wild-type channels reveals inward rectification at positive potentials. This rectification is probably due to block of NMDA channels by Mg^{2+} present in the cytoplasm of *Xenopus* oocytes. Since in a previous study of the effects of mutations in M2 on internal Mg^{2+} block we had found a strong correlation between the inward rectification of whole-cell currents and that of single-channel currents recorded in the presence of 4 mM internal Mg^{2+} (see Kupper *et al.* 1996, Fig. 3), it was tempting to use the inward rectification of the whole-cell currents of oocytes expressing wild-type or mutant channels as an indicator of the internal Mg^{2+} block.

To compare with this approach the extent of internal Mg^{2+} block in the four cases illustrated in Figs 1*A–D*, we arbitrarily normalized the I–V relations (in the Mg^{2+}-free external solution) to currents recorded at −100 mV (Fig. 1*F*). The inward rectification of the wild-type is attenuated in NR1–NR2A(N+1S), is absent in NR1(N0S)–NR2A (which has a nearly linear I–V relation), and the NR1(N0Q)–NR2A displays a (paradoxical) outward rectification.

The results presented in Fig. 1 suggest that the two asparagines proposed to form the selectivity filter of the NMDA channel affect differentially the block by internal Mg^{2+}: mutations in NR1(N0) seem to have a much stronger effect on the internal Mg^{2+} block, whereas mutations of NR2(N+1) primarily alter external Mg^{2+} block. However, as shown below, more detailed examination of internal Mg^{2+} block did not confirm this interpretation.

Internal Mg^{2+} block of wild-type and NR1–NR2A(N+1S) NMDA receptors at high positive potentials

Due to the high rates of blocking and unblocking reactions (Li-Smerin & Johnson, 1996*a*), internal Mg^{2+} induces an apparent reduction of the elementary conductance of NMDA channels at depolarized potentials. Our previous comparison of the effects of internal Mg^{2+} block on single-channel currents from wild-type and NR1–NR2A(N+1S) NMDA channels revealed little difference among these receptors with applied potentials up to +40 mV (Kupper *et al.* 1996). However, at more depolarized potentials, the amplitudes of the single-channel currents of the mutant started increasing whereas that of the wild-type steadily decreased. A possible

explanation of this upturn of the i–V relation in the mutant ('escape') is that the mutant channel has a higher Mg^{2+} permeability than the wild-type. Attempts to examine single-channel currents at highly depolarized potentials, where one would predict still greater 'escape' of the mutant current, were not successful due to the instability of the patches in this potential range. We resorted to macroscopic current recordings that allow much faster measurements (they require a few 3 s voltage ramps) and hence are more stable. The analysis of macroscopic currents required that one accounts for possible confounding changes of open probability superimposed on changes of single-channel conductance. Indeed the open probability of NMDA channels has been shown to be sensitive both to membrane potential (Nowak & Wright, 1992) and to internal Mg^{2+} (Li-Smerin & Johnson, 1996*b*).

The normalized single-channel and macroscopic current–voltage relationships for wild-type NR1–NR2A in the absence and presence of 4 mM internal Mg^{2+} are superimposed in Fig. 2*A*. In the absence of Mg^{2+}, the single-channel i–V relations, which were only constructed between −100 and +100 mV, are approximately linear. In contrast, the I–V relation of the macroscopic current shows an outward rectification that becomes quite marked at very positive potentials. In the presence of Mg^{2+}, both curves show the expected inward rectification in the low positive potential range but at higher positive potentials the macroscopic I–V relation turns outward like the curve obtained in 0 Mg^{2+}.

The divergence of the current–voltage curves obtained from measurements of single and macroscopic currents in the absence of Mg^{2+} is probably due to the voltage sensitivity of the open probability (Nowak & Wright, 1992). The difference between the two curves is relatively small, probably because the voltage sensitivity develops slowly (tens of seconds) and the depolarizing ramps are brief. Figure 2*B*, which quantifies the blocking effect of internal Mg^{2+} calculated from the data of Fig. 2*A*, shows an excellent agreement between the block deduced from the reduction of single-channel currents (□) and the block deduced from the reduction of macroscopic currents (noisy trace). This implies that, regardless of the mechanism of the macroscopic current outward rectification, this voltage dependence is unaffected by the presence of internal Mg^{2+}. Although this conclusion is strictly valid only for data obtained below +100 mV, where we demonstrate directly that the blocks are comparable, it is tempting to assume that it can be extended above +100 mV. Clearly the recording of a

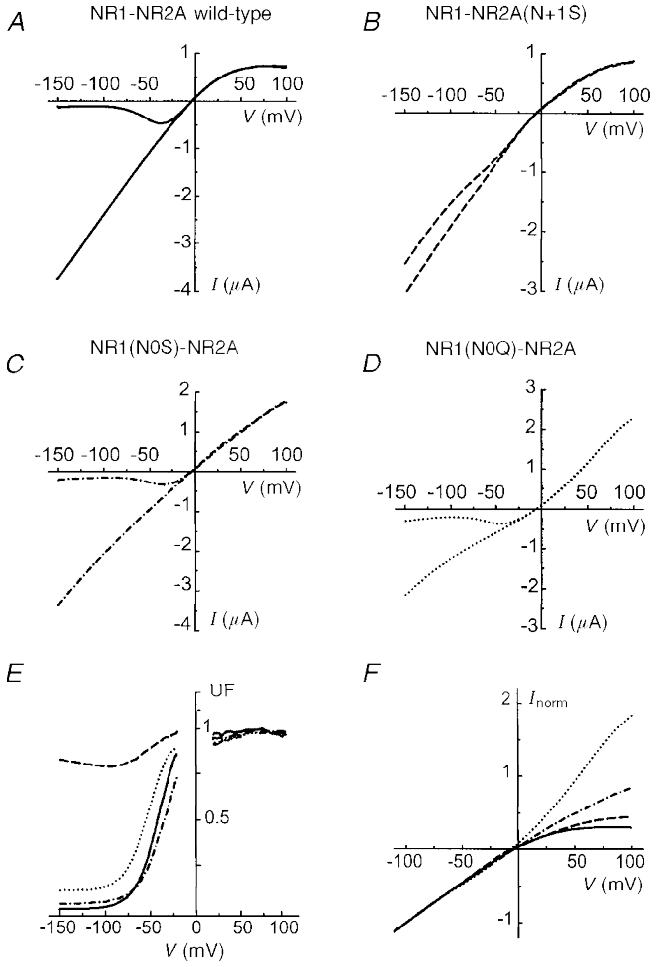

Figure 1. Whole-oocyte I–V relations of wild-type and mutant NMDA receptors. I–V relations were obtained in different oocytes expressing (wild-type) NR1–NR2A (*A*), NR1–NR2A(N+1S) (*B*), NR1(N0S)–NR2A (*C*) and NR1(N0Q)–NR2A (*D*) channels

A–*D*, I–V relations were built using 2 s ramps from −150 to +100 mV applied in the presence and in the absence of 100 μM glutamate. Each graph shows two such I–V relations obtained either in the absence of external Mg^{2+}, or in the presence of 100 μM external Mg^{2+}. Note that in the four cases, the external Mg^{2+} only affects inward currents, and that the outward currents are not affected. *E*, the block by external Mg^{2+} is evaluated by the ratio (unblocked fraction, UF) of the current recorded in the presence of external Mg^{2+} over the current recorded in the absence of external Mg^{2+}. *F*, the I–V relations of wild-type and mutant channels in the absence of external Mg^{2+} have been aligned by normalizing their current values to −100 mV. Continuous line, NR1–NR2A; - - -, NR1–NR2A(N+1S); - · - · -, NR1(N0S)–NR2A; · · · ·, NR1(N0Q)–NR2A.

significant macroscopic current at +200 mV demonstrates a finite channel conductance at this potential in the presence of internal Mg^{2+}.

Examination of the mutant NR1–NR2A(N+1S) in conditions similar to those of Fig. 2*A* and *B* reveals significant differences with the wild-type (Fig. 2*C* and *D*). Although the current–voltage curves obtained in the absence of Mg^{2+} are very similar to those of the wild-type, in the presence of Mg^{2+} and at high positive potentials (above +40 mV) a marked outward rectification ('escape') is seen.

The behaviour of the mutant channel illustrated in Fig. 2*C* and *D* cannot be described by the 'simplified' Woodhull model previously applied (Johnson & Ascher, 1990; Li-Smerin & Johnson, 1996*a*) since this model does not account for the persistence of current at very positive potentials. We therefore used a model that includes a permeation term (as in the original model proposed by Woodhull, 1973) and tested whether a simple change of this term could satisfactorily describe the effects of the NR2A(N+1S) mutation. For simplicity the three-barrier two-site energy profile was reduced to the structures assumed to control the effects of internal Mg^{2+} (i.e. the central and internal barriers and the energy well between them).

This simplified model requires six free parameters (three rate constants and three fractions of membrane field), that cannot be unambiguously deduced from a classical fitting of the UF curves. We chose to fit the UF curves approximately, adjusting each of the parameters successively. The initial values of the parameters k_{on}, δ_{on}, k_{off} and δ_{off} were set to the values calculated by Li-Smerin & Johnson (1996*a*). We then added, without an *a priori* constraint, two terms for Mg^{2+} permeation (k_{perm} and δ_{perm}). Using the values indicated in the legend of Fig. 2, we were able to model correctly the internal Mg^{2+} block of both wild-type channels (see Fig. 2*B*) and mutant channels (Fig. 2*D*) by changing only the value of k_{perm}. The values used for k_{on} and k_{off} at 0 mV were very similar to those obtained by Li-Smerin &

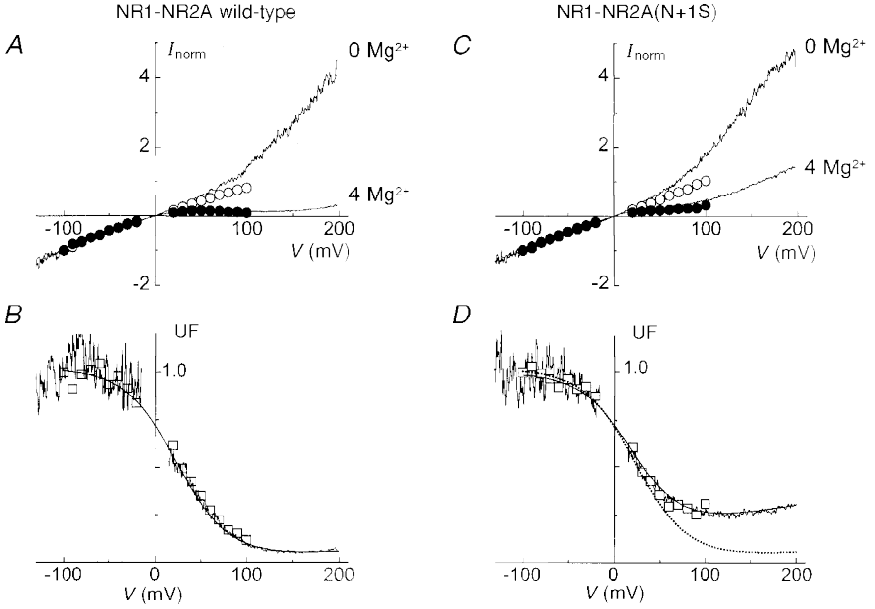

Figure 2. Internal Mg^{2+} block of (wild-type) NR1–NR2A and mutant NR1–NR2A(N+1S) channels

A and *C*, the *I–V* relations of macroscopic (continuous traces) and of single-channel currents (circles) of NR1–NR2A (*A*) and NR1–NR2A(N+1S) (*C*) channels were constructed in the absence (upper traces; ○) and in the presence (lower traces; ●) of 4 mM internal Mg^{2+}. All *I–V* relations were obtained in different outside-out patches and normalized to the current value at −100 mV. Macroscopic *I–V* relations were obtained during 3 s voltage ramps from −150 to +200 mV whereas single-channel *i–V* relations were obtained using voltage steps ranging between −100 and +100 mV. *B* and *D*, unblocked fraction of the current (UF) of NR1–NR2A (*B*) and NR1–NR2A(N+1S) (*D*) channels calculated from macroscopic currents (noisy trace) and from single-channel currents (□). Close to the reversal potential, UF takes artifactual values which have been blanked. The macroscopic UF curves were fitted with eqn (2) between −100 and +200 mV (continuous curve). In *D*, the theoretical UF curve of the wild-type data is replotted for comparison (dotted line). The values used for 5 of the 6 parameters were identical for the mutant and the wild-type ($k_{on} = 1{\cdot}8 \times 10^7$ M^{-1} s^{-1}; $k_{off} = 1{\cdot}75 \times 10^5$ s^{-1}; $\delta_{on} = 0{\cdot}3$; $\delta_{off} = 0{\cdot}15$; $\delta_{perm} = 0{\cdot}35$). The difference between the wild-type and the mutant was entirely accounted for by changing the value of k_{perm} from 2×10^3 s^{-1} in the wild-type to $1{\cdot}4 \times 10^4$ s^{-1} in the mutant.

Johnson (1996*a*). The values of δ_{on} and δ_{off} had to be increased (by 0·1 and 0·05, respectively) to account for the greater steepness of the block measured in our experiments. The value chosen for δ_{perm} was slightly larger than δ_{on}, to account for the mild upturn of the UF curve above +150 mV. The value of k_{perm} was then adjusted. The best fit of the data was obtained with a single change in parameters, namely a 7-fold increase in k_{perm} from 2×10^3 s^{-1} in the wild-type to $1{\cdot}4 \times 10^4$ s^{-1} in the mutant (Fig. 2*D*). This suggests that the major effect of the NR2A(N+1S) mutation on the internal Mg^{2+} block is a reduction of the height of the central barrier.

Internal Mg^{2+} block of NR1(N0Q)–NR2A channels

The whole-oocyte experiments suggested that the mutation NR1(N0Q) completely eliminates the inward rectification due to internal Mg^{2+} block and even introduces an outward rectification (Fig. 1*D*). To clarify these effects we analysed the NMDA currents in outside-out patches, measuring both single-channel currents at fixed potentials and macroscopic currents during voltage ramps on patches expressing a large number of channels. We were aware that the results obtained using the latter approach would be more difficult to interpret due to the existence of two conductance states in the NR1(N0Q) mutant channels and to the dependence of the relative probabilities of opening of each conductance state on the monovalent cations present on both sides of the membrane (Schneggenburger & Ascher, 1997). Furthermore the possibility had to be considered that the two states may be differentially sensitive to internal Mg^{2+}, in either their relative open probabilities or in their elementary conductances (in another mutant NMDA channel the two conductance states are differentially sensitive to external Mg^{2+}; Premkumar & Auerbach, 1996).

Representative single-channel recordings at −80 and +80 mV in the absence (left panels) and presence of 4 mM internal Mg^{2+} (right panels) are shown in Fig. 3*A*. In symmetrical Cs^+ (i.e. standard recording conditions) the open probabilities of the two conductance states are in the same range. Both the main and subconductance levels are strongly blocked by internal Mg^{2+} at positive membrane potentials; examination of the *i–V* relations of both conductances reveals a similar reduction of the main and subconductance currents by internal Mg^{2+} (Fig. 3*B* and *C*). The voltage dependence of the unblocked fractions of the two elementary currents confirms that the two conductance states of NR1(N0Q)–NR2A channels are blocked by

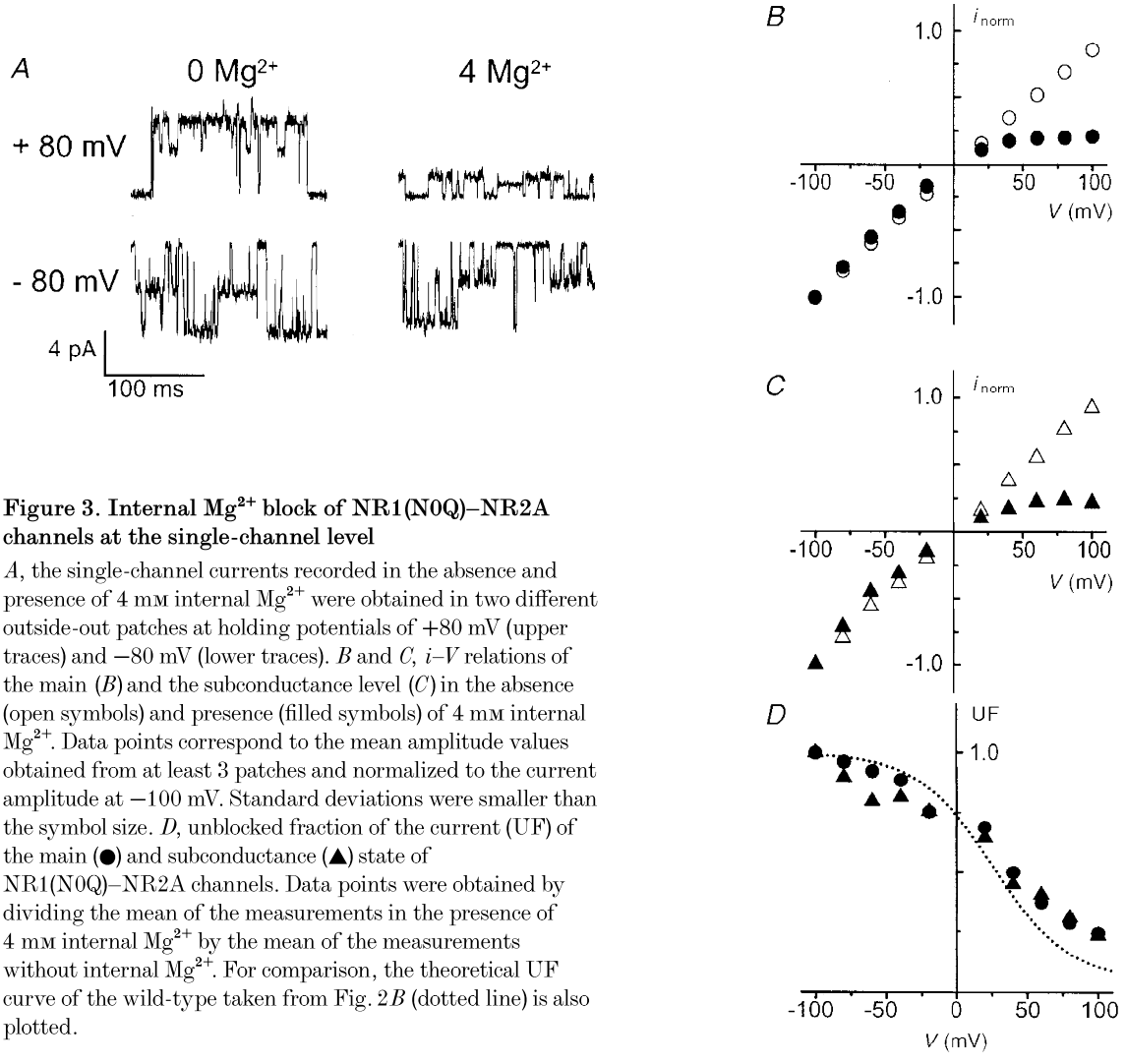

Figure 3. Internal Mg^{2+} block of NR1(N0Q)–NR2A channels at the single-channel level

A, the single-channel currents recorded in the absence and presence of 4 mM internal Mg^{2+} were obtained in two different outside-out patches at holding potentials of +80 mV (upper traces) and −80 mV (lower traces). *B* and *C*, *i–V* relations of the main (*B*) and the subconductance level (*C*) in the absence (open symbols) and presence (filled symbols) of 4 mM internal Mg^{2+}. Data points correspond to the mean amplitude values obtained from at least 3 patches and normalized to the current amplitude at −100 mV. Standard deviations were smaller than the symbol size. *D*, unblocked fraction of the current (UF) of the main (●) and subconductance (▲) state of NR1(N0Q)–NR2A channels. Data points were obtained by dividing the mean of the measurements in the presence of 4 mM internal Mg^{2+} by the mean of the measurements without internal Mg^{2+}. For comparison, the theoretical UF curve of the wild-type taken from Fig. 2*B* (dotted line) is also plotted.

internal Mg^{2+} to the same extent and with the same apparent affinity (Fig. 3*D*). The internal Mg^{2+} block of the mutant channels is not significantly different from that of wild-type channels for holding potentials up to +40 mV (see dotted line, replotted from Fig. 2*C*). Above this potential, however, the block of mutant channels is smaller than that of wild-type channels. For example, at +100 mV the UF of the mutant channels is close to 25% whereas the UF of wild-type channels is 12% (Fig. 2*C*). Note that the UF value in the mutant NR1(N0Q)–NR2A compares well with that of the mutant NR1–NR2(N+1S) at +100 mV (29%, Fig. 2*D*).

Thus, at the single-channel level, the block of the mutant NR1(N0Q)–NR2A by internal Mg^{2+} differs from that of the wild-type only in the high positive potential range, and in this resembles the block analysed in the mutant NR1–NR2A(N+1S). To further assess this similarity we extended the *I–V* relation in a more depolarized range by analysing the macroscopic NMDA currents of patches expressing a large number of receptors. In these experiments, 100 μM EDTA was included in the external solution to remove trace Ca^{2+} and Ba^{2+}, as these ions block the NR1(N0Q)–NR2A channels with high apparent affinity (see Methods). Under these conditions the macroscopic NR1(N0Q)–NR2A *I–V* curves in the absence of internal Mg^{2+} are nearly linear (Fig. 4*A*). After inclusion of 4 mM Mg^{2+} in the internal solution the current rectifies inwards at moderately depolarized potentials and then outwards at potentials more positive than +100 mV. These results extend and confirm those obtained from single-channel recording: in the mutant NR1(N0Q)–NR2A strong depolarization reveals a substantial current 'escape' from the internal Mg^{2+} block.

The comparison of the *I–V* relations available (i.e. those of the two elementary conductances (Fig. 3), that of the macroscopic current in an outside-out patch (Fig. 4*A*) and that of the whole oocyte (Fig. 1) reveals two additional discrepancies. First, the *I–V* relation of the macroscopic current (outside-out patch) differs from that obtained from whole-oocyte recordings. Second the *I–V* relationship obtained for the macroscopic current also differs from those obtained from the analysis of the single-channel conductance states.

We examined if the first discrepancy could result from differences in the ionic composition of the solutions in the two types of recording conditions. The macroscopic (outside-out) current recordings had employed symmetrical solutions, with the same concentration of Cs^+ ions in the pipette and in the bath solution; in the whole-oocyte recordings the monovalent cations were different outside and inside. As it is known that asymmetrical monovalent cation solutions modify the open probabilities of the two conductance states of NR1(N0Q)–NR2A channels (Schneggenburger & Ascher, 1997), we examined the *I–V* curves obtained from macroscopic patch recordings under conditions that better

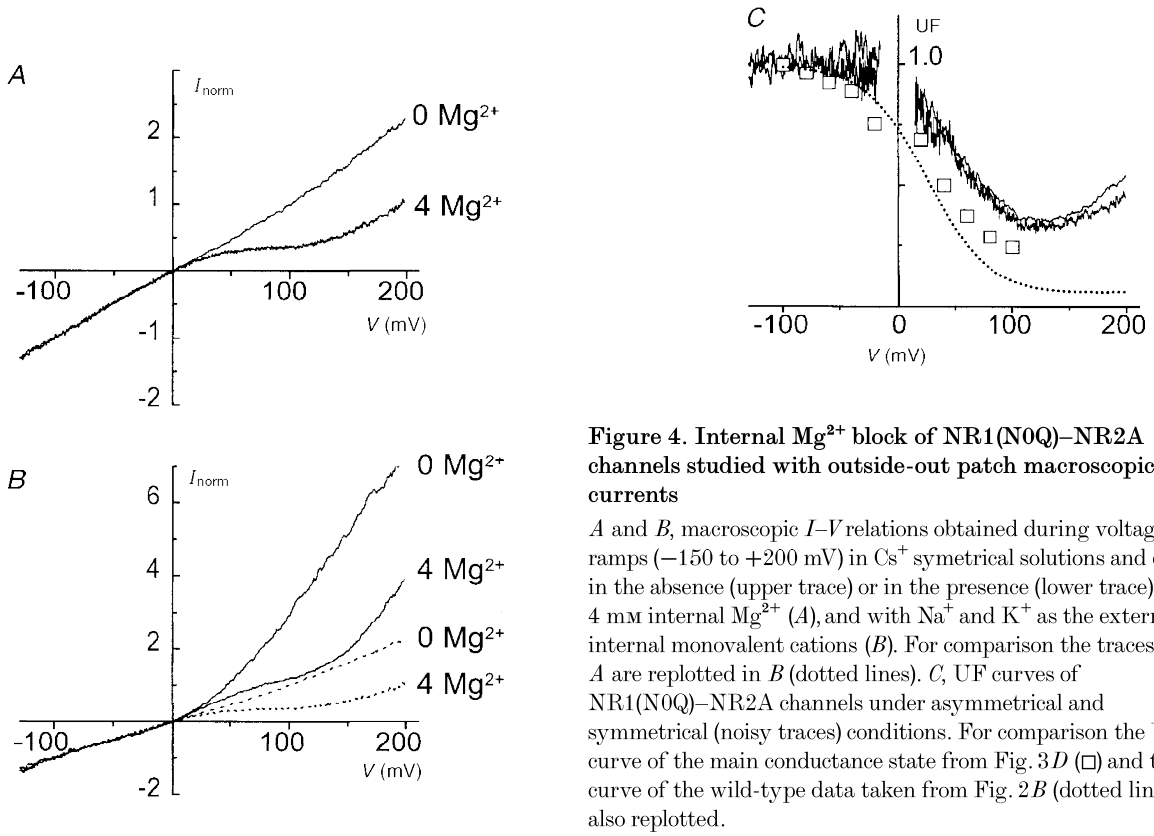

Figure 4. Internal Mg^{2+} block of NR1(N0Q)–NR2A channels studied with outside-out patch macroscopic currents

A and *B*, macroscopic *I–V* relations obtained during voltage ramps (−150 to +200 mV) in Cs^+ symetrical solutions and either in the absence (upper trace) or in the presence (lower trace) of 4 mM internal Mg^{2+} (*A*), and with Na^+ and K^+ as the external and internal monovalent cations (*B*). For comparison the traces from *A* are replotted in *B* (dotted lines). *C*, UF curves of NR1(N0Q)–NR2A channels under asymmetrical and symmetrical (noisy traces) conditions. For comparison the UF curve of the main conductance state from Fig. 3*D* (□) and the UF curve of the wild-type data taken from Fig. 2*B* (dotted line) are also replotted.

mimick the ionic distributions existing in the whole-oocyte recordings. With asymmetrical solutions (Na^+_o–K^+_i) and in the absence of internal Mg^{2+}, the *I–V* relation exhibits a marked outward rectification (Fig. 4*B*). In the presence of internal Mg^{2+} this rectification is reduced by the opposing effect of the internal Mg^{2+}, which tends to produce inward rectification. Thus, although the outward rectification is still detectable at very positive potentials, the *I–V* of the macroscopic current is now nearly linear in the range −100 to +100 mV, and in this range very similar to the one observed in the whole oocyte (compare Fig. 4*B* with Fig. 1*D*). Thus the 'linearity' of the *I–V* relationship obtained from whole-oocyte currents is probably the net result of two opposing voltage-dependent processes occurring at positive potentials: a voltage-dependent increase in the channel open probability masks the inward rectification due to internal Mg^{2+} block.

The internal Mg^{2+} UF curves calculated from the macroscopic patch currents recorded under either symmetrical Cs^+ (Fig. 4*A*) or asymmetrical Na^+_o–K^+_i conditions (Fig. 4*B*) are shown superimposed in Fig. 4*C*. The plots are nearly identical, which indicates that, although the transmembrane distribution of monovalent cations influences the probability of opening of the channels, it does not affect substantially the block by internal Mg^{2+}.

The asymmetry in the ionic composition of external and internal solutions does not explain the second discrepancy between the *I–V* relations, namely that, in identical (symmetrical) ionic conditions, the single-channel currents (Fig. 4*C*, □) showed more block by internal Mg^{2+} than the macroscopic current (Fig. 4*C*, continuous lines), in particular over the range between +20 and +100 mV. It appears that, in the NR1(N0Q)–NR2A mutant, internal Mg^{2+} not only reduces the single-channel current but also modulates, in a voltage-dependent manner, the gating of the channels.

To test whether internal Mg^{2+} modulates NR1(N0Q)–NR2A mutant channels by altering P_M/P_S, the ratio of the open probabilities of the two (main and sub-) conductance states, we examined all point histograms of single-channel records obtained at two holding potentials (−60 and +60 mV) in the absence and presence of 4 mM internal Mg^{2+}. The areas of the individual Gaussian curves fitted to the amplitude histograms were measured for each open state (main and substates). The ratio of the probabilities that the channel is in one of the two open states (P_M and P_S) was then calculated as the ratio of the corresponding areas. In the example shown in Fig. 5, in the absence of internal Mg^{2+} (Fig. 5*A*), the P_M/P_S ratio at +60 mV is about 1·6-fold larger than that obtained at −60 mV (consistent with depolarization increasing the probability of the mutant channel to reside in the main state). However, in the presence of 4 mM internal Mg^{2+} the P_M/P_S ratio at +60 mV is about 4·1-fold larger than that obtained at −60 mV (Fig. 5*B*), indicating that internal Mg^{2+} increased by about 2·6-fold the relative occupancy of the main conductance state at +60 mV.

We repeated the analysis of the relative occupancies of sub- and main conductance states in seven patches (three in internal Mg^{2+}-free solution, four in the presence of internal Mg^{2+}); approximately the same change in the P_M/P_S ratios was seen in all cases (0 Mg^{2+}, 1·7 ± 0·09; 4 mM Mg^{2+}, 3·8 ± 1·6). Despite the relatively limited sample number and the brief duration of the records analysed (a few seconds), we interpret the results as providing strong support for an effect of internal Mg^{2+} on the gating of NR1(N0Q)–NR2A channels. An increase in the relative open probability of the main state can qualitatively explain the discrepancy between the block of the single-channel current and that of macroscopic current (see Fig. 4*C*). The data do not exclude the possibility that internal Mg^{2+} has yet other effects, such as a decrease in the closed probabilities.

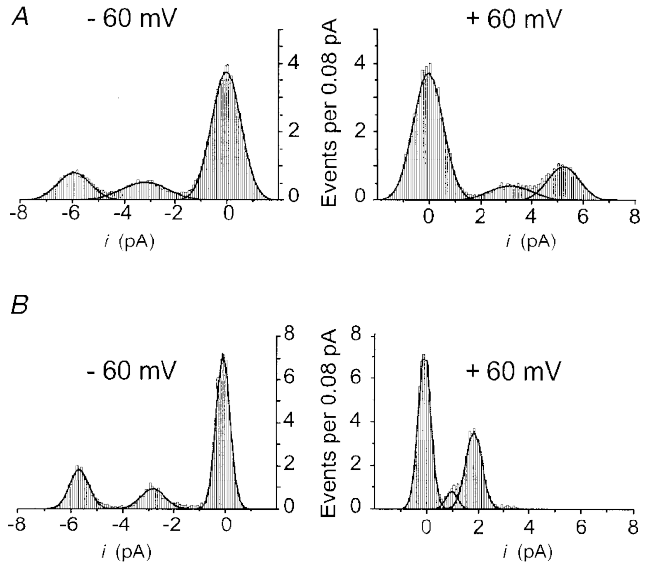

Figure 5. Internal Mg^{2+} affects the gating properties of NR1(N0Q)–NR2A channels

All point histograms from two different outside-out patches in the absence (*A*) and presence (*B*) of 4 mM internal Mg^{2+}. The holding potential was −60 mV (left panels) and + 60 mV (right panels). The length of the recordings used to construct these histograms varied between 3·6 and 7·5 s. The best fits were obtained using eqn (1) (see Methods) with the following parameters for peaks 1, 2 and 3 corresponding to the main, sub- and closed states, respectively. −60 mV, 0 Mg^{2+}: $x_1 = -5{\cdot}94$, $w_1 = 1{\cdot}25$, $A_1 = 1{\cdot}25$, $x_2 = -3{\cdot}2$, $w_2 = 1{\cdot}81$, $A_2 = 1{\cdot}19$, $x_3 = -0{\cdot}02$, $w_3 = 1{\cdot}13$, $A_3 = 5{\cdot}36$; +60 mV, 0 Mg^{2+}: $x_1 = 5{\cdot}24$, $w_1 = 1{\cdot}23$, $A_1 = 1{\cdot}52$, $x_2 = 3{\cdot}18$, $w_2 = 1{\cdot}71$, $A_2 = 0{\cdot}92$, $x_3 = -0{\cdot}04$, $w_3 = 1{\cdot}14$, $A_3 = 5{\cdot}36$; −60 mV, 4 mM Mg^{2+}: $x_1 = -5{\cdot}67$, $w_1 = 0{\cdot}73$, $A_1 = 1{\cdot}67$, $x_2 = -2{\cdot}82$, $w_2 = 0{\cdot}94$, $A_2 = 1{\cdot}08$, $x_3 = -0{\cdot}07$, $w_3 = 0{\cdot}54$, $A_3 = 4{\cdot}88$; +60 mV, 4 mM Mg^{2+}: $x_1 = 1{\cdot}83$, $w_1 = 0{\cdot}64$, $A_1 = 2{\cdot}84$, $x_2 = 0{\cdot}96$, $w_2 = 0{\cdot}44$, $A_2 = 0{\cdot}45$, $x_3 = -0{\cdot}08$, $w_3 = 0{\cdot}48$, $A_3 = 4{\cdot}39$.

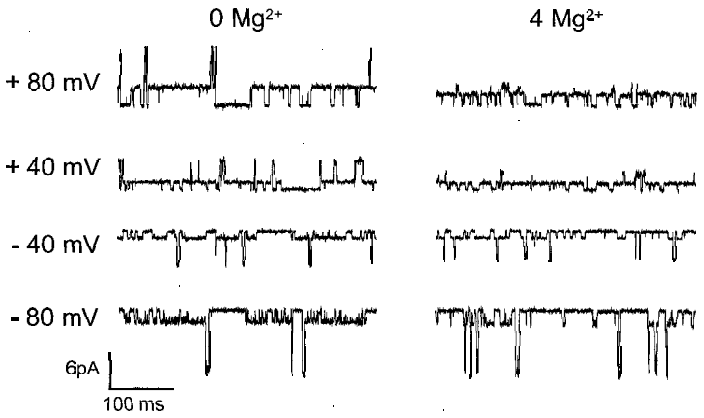

Figure 6. Internal Mg^{2+} block of NR1(N0S)–NR2A channels at the single-channel level

Representative single-channel recordings in the absence (left panels) and presence of 4 mM internal Mg^{2+} (right panels) obtained in two different outside-out patches. Holding potentials are indicated to the left of the current traces.

Internal Mg^{2+} block of NR1(N0S)–NR2A channels

Previous studies had not examined the sensitivity of NR1(N0S)–NR2A channels to either internal or external Mg^{2+} block. Judging from the *I–V* curve obtained from whole oocytes in the presence and absence of internal Mg^{2+} (see Fig. 1*C*), these mutant channels appeared less sensitive to block by internal Mg^{2+} than the wild-type NR1–NR2A channels. Wollmuth *et al.* (1996) had shown that the permeability of NR1(N0S)–NR2A channels to organic cations is very similar to that of the wild-type. A reduced internal Mg^{2+} block could indicate that different steric factors control the permeability of organic cations and Mg^{2+} ions.

Single-channel recordings were obtained from patches containing NR1(N0S)–NR2A channels in the absence and presence of internal Mg^{2+} (Figs 6 and 7). Like the NR1(N0Q)–NR2A channels, the NR1(N0S)–NR2A channels frequently enter a clearly discernible subconductance state. The main conductance rectifies slightly inward whereas the subconductance rectifies outward. Furthermore, internal Mg^{2+} does not reduce the two conductances in the same manner. As can be seen in the right panel of Fig. 6, at positive potentials the main conductance is much more reduced than the subconductance. The *i–V* relations of the main and the subconductance states in the absence (open symbols) and presence (filled symbols) of internal Mg^{2+} are

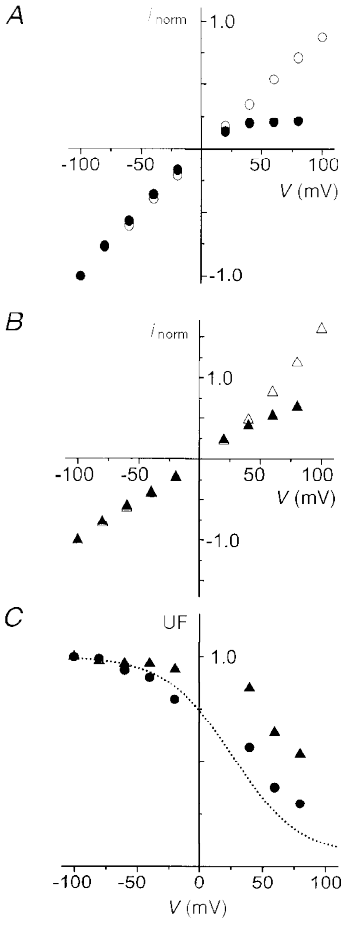

Figure 7. NR1(N0S)–NR2A channels

A and *B*, *i–V* relations of the main (*A*) and the subconductance level (*B*) in the absence (open symbols) and presence (filled symbols) of 4 mM internal Mg^{2+}. Data points correspond to the mean of measurements obtained from at least 3 patches (the standard deviations are smaller than the symbol size). They are normalized to the current value at −100 mV. *C*, UF curves of the main (●) and subconductance (▲) states of NR1(N0S)–NR2A channels. Data points were obtained by dividing the mean of the measurements in presence of 4 mM internal Mg^{2+} by the mean of the measurements in the absence of internal Mg^{2+}.

displayed in Fig. 7*A* and *B*. Figure 7*C* shows the fraction of the unblocked currents of the main conductance (circles) and the subconductance (triangles). In the voltage range where the block of the two conductances can be clearly separated, from +40 to +80 mV, internal Mg^{2+} blocks the subconductance less than the main conductance. The difference was found to be statistically significant by comparing the UF values measured at +60 mV ($UF_{main} = 0{\cdot}36 \pm 0{\cdot}04$, $n = 5$; $UF_{sub} = 0{\cdot}61 \pm 0{\cdot}07$, $n = 5$; different with $P > 95\%$) with the adapted Student's t test used in our previous study (Kupper *et al.* 1996).

DISCUSSION

This study was initiated on the basis of whole-cell voltage-clamp data which suggested that mutations of the NR2(N+1) asparagine affect mostly the external Mg^{2+} block, whereas mutations of the NR1(N0) asparagine affect more the internal Mg^{2+} block. However, single-channel data revealed that the internal block is affected in a similar way by mutations of NR1(N0) and NR2(N+1).

We shall first discuss the reasons for the discrepancies between macroscopic and single-channel currents, and then examine if our results can be integrated in a coherent picture of the channel structures involved in Mg^{2+} block.

Discrepancies between macroscopic and single-channel data

Discrepancies between the I–V relations measured under single-channel and macroscopic current conditions are expected from the fact that the macroscopic currents represent the product $NP_o i$, where N is the number of channels, P_o the probability that a channel be open at a given time and i the elementary current. In 1992, Nowak and Wright described a time- and voltage-dependent change in NP_o which occurred in outside-out patches and in the absence of internal Mg^{2+}. More recently, Li-Smerin & Johnson (1996*b*) showed that, in addition, internal Mg^{2+} produces an increased frequency of burst openings which makes the fractional block of the mean current (integrated over a few minutes) smaller than that of the single-channel current.

In our experiments using either the wild-type or the mutant NR1–NR2A(N+1S) channels, neither of the effects described by Nowak & Wright (1992) or by Li-Smerin & Johnson (1996*b*) were very marked, possibly (as pointed out in the Results section) because we used relatively fast voltage ramps. On the other hand, in the mutant NR1(N0Q)–NR2A, the inhibitory effect of internal Mg^{2+} is clearly greater for the single-channel current than for the macroscopic current, and the difference increases with depolarization (see Fig. 4*C*). Figure 5 shows that this change involves a change in the ratio of the open probabilities of the two conductance states. This introduces a major restriction in the interpretation of macroscopic current traces and reinforces the warning issued by Li-Smerin & Johnson (1996*b*) when they showed in native channels that internal Mg^{2+} influenced the voltage dependence of the NMDA current.

Distinguishing the Mg^{2+} barrier from the Mg^{2+} binding sites with mutant channels

We started this study with the simple assumption that, if a three-barrier two-site Mg^{2+} energy profile correctly described the NMDA channel (Johnson & Ascher, 1990; Li-Smerin & Johnson, 1996*a*), comparing the effects of a mutation on the external and internal Mg^{2+} blocks should allow one to decide if the mutation modifies one of the two Mg^{2+} binding sites and/or alters the central Mg^{2+} barrier. A change of one of the binding sites should affect differentially the external and internal Mg^{2+} blocks. Modifying the central barrier should affect similarly the permeation of both external and internal Mg^{2+} and, as a consequence, both external and internal Mg^{2+} blocks.

The main effects of the NR1(N0Q) and NR1(N0S) mutations can be accounted for by assuming that they lower the central barrier. Such a reduction would explain the mild reduction of the internal Mg^{2+} block, at least for NR1(N0Q) and for the main conductance state of the NR1(N0S) mutant. A lowering of the central barrier may also account for the reduced block by external Mg^{2+} first reported by Burnashev *et al.* (1992) and for the small escape observed in the external Mg^{2+} UF curves of the NR1 mutant channels at very negative voltages (in particular for NR1(N0Q), see Fig. 1*E*). However this moderate change in Mg^{2+} energy profile provides no explanation for the presence of a stable subconductance state in NR1(N0) mutant channels, and does not explain why internal Mg^{2+} produces a small rightward shift of the UF curve of this conductance in NR1(N0S)–NR2A.

The effects of the NR2A(N+1S) mutation require more than a lowering of the central barrier. The mutation increases the 'escape' for both internal Mg^{2+} (at positive potentials; see Fig. 2*B*) and for external Mg^{2+} (at negative potentials; see Fig. 1*E*) and it increases the permeability to dimethylammonium and diethylammonium (Wollmuth *et al.* 1996). Although each of these effects could be separately explained by a lowering of the central barrier, which may result for example from the widening of the selectivity filter (Wollmuth *et al.* 1996), a single change of k_{perm} would not explain why the mutation reduces the external Mg^{2+} block so much more than the internal one. It is therefore tempting to consider that the asparagine NR2(N+1) participates not only to the central barrier (like the asparagine NR1(N0)) but also to the external Mg^{2+} binding site and/or to the external Mg^{2+} barrier. The multiplicity of the effects induced by a substitution of this asparagine may mean that the mutation has long range effects on the structure of the channel, but it may also mean that the external barrier and the central barrier are physically very close inside the channel.

Although a Woodhull model such as the one used in Fig. 2 describes well the internal Mg^{2+} block of both wild-type and

mutant channels, and although such a model can also describe the external Mg^{2+} block (Ascher & Nowak, 1988; Jahr & Stevens, 1990), the two descriptions cannot be made by using the same parameters. This is immediately obvious if one considers the values of the δ: the sum of the values used for the internal block ($\delta_{perm} = 0{\cdot}35$, $\delta_{off} = 0{\cdot}15$, $\delta_{on} = 0{\cdot}3$) would push the central barrier towards the external side of the channel, a position which cannot explain the voltage dependence of the external Mg^{2+} block (Ascher & Nowak, 1988). This problem ('crossing of the δ's') has already been mentioned in the initial description of the internal Mg^{2+} block (Johnson & Ascher, 1990; see also Li-Smerin & Johnson, 1996*a*) and is evidently aggravated if one assumes permeation of the blocking ion and takes into account the voltage dependence of this permeation.

The fact that the Woodhull model cannot describe simultaneously (with a single set of values) both the internal and the external Mg^{2+} block probably indicates that some of the assumptions of the model are not valid. Three possibilities seem particularly worth exploring: (1) ion–ion interactions between the permeant and permeant-blocking ions have to be considered (Johnson & Ascher, 1990; Ruppersberg, von Kitzing & Schoepfer, 1994; Zarei & Dani, 1995; Li-Smerin & Johnson, 1996*a*; Premkumar & Auerbach, 1996; Sharma & Stevens, 1996) (for example, the apparent height of the central barrier in the Woodhull model may be partly controlled by occupancy in a neighbouring well, and thus depend on the affinity of permeant ions for their internal binding site). (2) k_{on} may become diffusion-limited at high voltages. This may strongly affect both the voltage dependence and the value of k_{perm} at 0 mV. (3) In an enlarged channel (as is the case for NR1(N0) and NR2A(N+1) mutant channels; see Wollmuth *et al.* 1996) the single file behaviour may partially break down and the apparent 'escape' may be due to a residual monovalent cation conductance in a Mg^{2+}-occupied channel (as seems to happen for Zn^{2+} block in Na^{+} channels; Schild & Moczydlowski, 1994).

Ascher, P. & Nowak, L. M. (1988). The role of divalent cations in the *N*-methyl-D-aspartate responses of mouse central neurones in culture. *Journal of Physiology* **399**, 247–266.

Béhé, P., Stern, P., Wyllie D. J., Nassar, M., Schoepfer, R. & Colquhoun, D. (1995). Determination of NMDA NR1 subunit copy number in recombinant NMDA receptors. *Proceedings of the Royal Society* B **262**, 205–213.

Bers, D., Patton, C. & Nuccitelli, R. (1994). A practical guide to the preparation of Ca buffers. *Methods in Cell Biology* **40**, 3–29.

Bertrand, D., Cooper, E., Valera, S., Rungger, D. & Ballivet, M. (1991). Electrophysiology of neuronal nicotinic acetylcholine receptors expressed in *Xenopus* oocytes following nuclear injection of genes or cDNAs. *Methods in Neuroscience* **4**, 174–193.

Burnashev, N., Schoepfer, R., Monyer, H., Ruppersberg, J. P., Günther, W., Seeburg, P. H. & Sakmann, B. (1992). Control by asparagine residues of calcium permeability and magnesium blockade in the NMDA receptor. *Science* **257**, 1415–1419.

Jahr, C. E. & Stevens, C. F. (1990). Voltage dependence of NMDA-activated macroscopic conductances predicted by single-channel kinetics. *Journal of Neuroscience* **10**, 3178–3182.

Johnson, J. W. & Ascher, P. (1990). Voltage-dependent block by intracellular Mg^{2+} of *N*-methyl-D-aspartate-activated channels. *Biophysical Journal* **57**, 1085–1090.

Kuner, T., Wollmuth, L., Karlin, A., Seeburg, P. H. & Sakmann, B. (1996). Structure of the NMDA receptor channel M2 segment inferred from the accessibility of substituted cysteines. *Neuron* **17**, 343–352.

Kupper, J., Ascher, P. & Neyton, J. (1996). Probing the pore region of recombinant *N*-methyl-D-aspartate channels using external and internal magnesium block. *Proceedings of the National Academy of Sciences of the USA* **93**, 8648–8653.

Li-Smerin, Y. & Johnson, J. W. (1996*a*). Kinetics of the block by intracellular Mg^{2+} of the NMDA-activated channel in cultured rat neurons. *Journal of Physiology* **491**, 121–135.

Li-Smerin, Y. & Johnson, J. W. (1996*b*). Effects of intracellular Mg^{2+} on channel gating and steady state responses of the NMDA receptor in cultured rat neurons. *Journal of Physiology* **491**, 137–150.

Mayer, M. L., Westbrook, G. L. & Guthrie, P. B. (1984). Voltage-dependent block by Mg^{2+} of NMDA responses in spinal cord neurones. *Nature* **309**, 261–263.

Mori, H., Masaki, H., Yamakura, T. & Mishina, M. (1992). Identification by mutagenesis of a Mg^{2+}-block site of the NMDA receptor channel. *Nature* **358**, 673–675.

Nowak, L. M., Bregestovski, P., Ascher, P., Herbet, A. & Prochiantz, A. (1984). Magnesium gates glutamate-activated channels in mouse central neurones. *Nature* **307**, 462–465.

Nowak, L. M. & Wright, J. M. (1992). Slow voltage-dependent changes in channel open-state probability underlie hysteresis of NMDA responses in Mg^{2+}-free solution. *Neuron* **8**, 181–187.

Premkumar, L. S. & Auerbach, A. (1996). Identification of a high affinity divalent cation binding site near the entrance of the NMDA receptor channel. *Neuron* **16**, 869–880.

Ruppersberg, J. P., Mosbacher, J., Günther, W., Schoepfer, R. & Falker, B. (1993). Studying block in cloned *N*-methyl-D-aspartate (NMDA) receptors. *Biochemical Pharmacology* **47**, 1877–1885.

Ruppersberg, J. P., von Kitzing, E. & Schoepfer, R. (1994). The mechanism of magnesium block of NMDA receptors. *Seminars in Neurosciences* **6**, 87–96.

Sakurada, K., Masu, M. & Nakanishi, S. (1993). Alteration of Ca^{2+} permeability and sensitivity to Mg^{2+} and channel blockers by a single amino acid substitution in the *N*-methyl-D-aspartate receptor. *Journal of Biological Chemistry* **268**, 410–415.

Schild, L. & Moczydlowski, E. (1994). Permeation of Na^{+} through open and Zn^{2+}-occupied conductance states of cardiac sodium channels modified by batrachotoxin: exploring ion-ion interactions on a multi-ion channel. *Biophysical Journal* **66**, 654–666.

Schneggenburger, R. & Ascher, P. (1997). Coupling of permeation and gating in an NMDA-channel pore mutant. *Neuron* **18**, 167–177.

Sharma, G. & Stevens, C. F. (1996). Interactions between two divalent ion binding sites in *N*-methyl-D-aspartate receptor channels. *Proceedings of the National Academy of Sciences of the USA* **93**, 14170–14175.

Wollmuth, L. P., Kuner, T., Seeburg, P. H. & Sakmann, B. (1996). Differential contribution of the NR1- and NR2A-subunits to the selectivity filter of recombinant NMDA receptor channels. *Journal of Physiology* **491**, 779–797.

Woodhull, A. M. (1973). Ionic blockade of sodium channels in nerve. *Journal of General Physiology* **61**, 687–708.

Zarei, M. M. & Dani, J. A. (1995). Structural basis for explaining open-channel blockade of the NMDA receptor. *Journal of Neuroscience* **15**, 1446–1454.

Acknowledgements

We thank John Dempster for the Strathclyde Electrophysiology Software Package and Chris Patton for the WinMaxc program. We also thank Boris Barbour, Jon Johnson, Lorna Role, Rod MacKinnon and Ralf Schneggenburger for their comments. This work was supported by a fellowship from the Human Frontiers Science Program (J.K.) and a grant from the European Community (BIO 2-CT93-0243).

Corresponding author

J. Neyton: Laboratoire de Neurobiologie (URA CNRS 1857) Ecole Normale Supérieure, 46 rue d'Ulm, 75005 Paris, France.

Authors' email addresses

J. Kupper: kupper@biochem.mpg.de

P. Ascher: pascher@wotan.ens.fr

J. Neyton: neyton@wotan.ens.fr

Author's present address

J. Kupper: Department of Membrane- and Neurophysics, Max Planck Institute for Biochemistry, Am Klopferspitz 18a, 82152 Martinsried, Germany.